Zajac, W.; Tarach, M.; Trenczek-Zajac, A. (2017). Towards control over redox behaviour and ionic conductivity in LiTi2(PO4)(3) fast lithium-ion conductor. Acta Materialia. 140:417-423. doi:10.1016/j.actamat.2017.08.064

Elsevier Editorial System(tm) for Acta Materialia

Manuscript Draft

Manuscript Number: A-17-2093R1

Title: Towards control over redox behaviour and ionic conductivity in LiTi2(PO4)3 fast lithium-ion conductor

Article Type: Full length article

Keywords: Electroceramics; Superionic conductor; Electrode potential; Optical spectroscopy; Li-ion battery

Corresponding Author: Dr. Wojciech Zajac,

Corresponding Author's Institution: AGH University of Science and Technology, Faculty of Energy and Fuels

First Author: Wojciech Zajac

Order of Authors: Wojciech Zajac; Mateusz Tarach; Anita Trenczek-Zając

Abstract: The location of redox couples in transition metal compounds is among the key factors that determine their applicability. AM2(PO4)3 NASICONs (A = Na, Li; M = Ti, Zr, Hf, Ge, Sn, Fe, ...) form an intriguing group that feature fast ion diffusion and tunable reduction/oxidation potentials and can therefore find numerous applications. The present study focuses on the LiTi2(PO4)3 member of this family and the possibility of controlling its transport and redox properties. It highlights the close relationship between the modification of the crystal and band structures via substitutions in the Ti sublattice or intercalation with lithium and its redox behaviour as well as transport properties. The correlation between ionic conductivity and the position of the Ti4+/Ti3+ redox potential is discussed. UV-VIS reflectance spectra revealed a significant impact of the type of dopant as well as the level of intercalation on the position of the fundamental absorption edge, indicating the possibility of modifying the electronic structure. In the case of some of the examined dopants (Nb, Sn, In), more complex interaction was observed, since they introduce their own redox activity, and thus enable the material's behaviour to be modified even further.

Cover Letter

Dear Editor,

We hereby submit corrected manuscript entitled „Towards control over redox behaviour and ionic conductivity in $LiTi_2(PO_4)_3$ fast lithium-ion conductor" to be considered for publication in Acta Materialia.

All suggestions made by the reviewer were accepted and appropriate changes were introduced to the text. Changes in the manuscript were highlighted in yellow.

Sincerely,

Wojciech Zajac, Ph.D.

***Response to Reviewer**

Reviewer #1: In this article, the authors investigated the relationship between the modification of the crystal and band structures via substitutions in the Ti sublattice or intercalation with lithium and its redox behavior as well as transport properties. The manuscript shows rigorous scientificity and provides good theoretical support about studying the applicability of NASICON-type compounds. It is basically interesting and worth to be considered for publication after minor revisions. But, there are several points that the authors should address and/or clarify:

1. **As shown in Fig.6a, there are two reduction peaks for $Li_{0.7}Ti_{1.7}Nb_{0.3}(PO_4)_3$ between 2.0 V and 2.8 V, however, others are only one reduction peaks. How to explain it?**

Generally, for NASICONs lithium insertion proceeds via a two-phase mechanism, as described in equation (2) in the manuscript. This stands behind constant potential vs. reference related to the Ti^{4+}/Ti^{3+} redox couple, as usually observed for $LiTi_2(PO_4)_3$. Conversely, it seems that for $Li_{0.7}Ti_{1.7}Nb_{0.3}(PO_4)_3$, beside Ti^{4+}/Ti^{3+}, another redox process appeared. We guess that it could be related to partial substitution of titanium with niobium and introduction of Nb^{5+}/Nb^{4+} ($Nb^{5+} + e^- = Nb^{4+}$) reduction process. We were not able to find any reports on redox processes related to Nb in the NASICON structure to support this statement, however, Patoux and Masquelier (Chem. Mater. 2002, 14, 2334-2341) showed that potential of lithium insertion into $NbPO_5$ coupled with Nb^{5+}/Nb^{4+} pair could be close to 2 V vs. Li^+/Li, which makes our guess plausible.
This explanation was included in page 11 of the manuscript.

2. **The $LiTi_2(PO_4)_3$ exhibits a typical two-phase mechanism as clearly shows in Fig.4 via chemical reaction of $LiTi_2(PO_4)_3$ with n-butyllithium. But what I am interested in is that the phase change via electrochemical lithiation process.**

Patoux and Masquelier (Chem. Mater. 2002, 14, 5057-5068) clearly demonstrated a two-phase mechanism of electrochemical insertion of lithium to $LiTi_2(PO_4)_3$, as presented below:

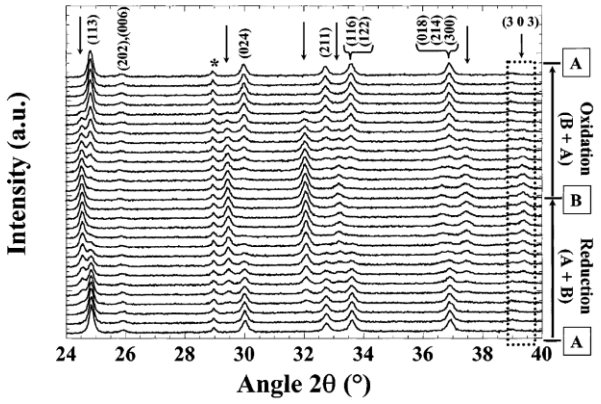

Figure 13. Evolution of the in situ X-ray diffraction patterns of an electrode of $LiTi_2(PO_4)_3$ during the first cycle under a GITT mode between 3.40 and 2.00 V vs Li^+/Li. Acquisition time of 1.5 h in the 20.00−42.00 2θ (°) window from a Cu Kα radiation on a Scintag diffractometer. The peak positions of the growing second phase are indicated by vertical arrows. The asterisk indicates a diffraction peak of the hardware.

Patoux and Masquelier (Chem. Mater. 2002, 14, 5057-5068)

Our preliminary investigations including *in situ* X-ray diffraction measurements on electrochemically lithiated $LiTi_2(PO_4)_3$ (not included in the manuscript), confirmed two phase type of mechanism for the electrochemical lithiation process, similarly as reported by Patoux and Masquelier:

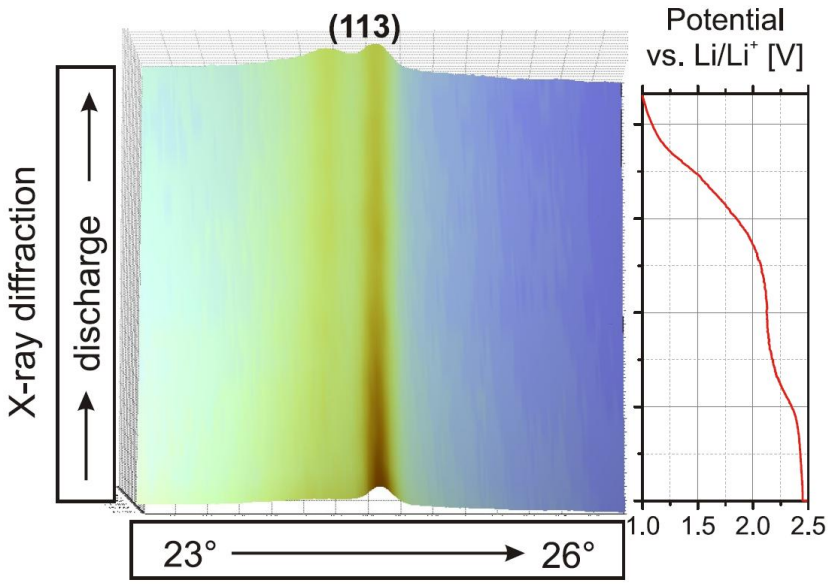

Our result. Not published.

To avoid any confusions, we slightly amended the text of the manuscript (page 9, lines 17-39).

3. **There are some format/grammar errors in the manuscript, Please check through the full manuscript and revised them. For example:**

   "Building on that knowledge, numerous polyanionic framework structures were proposed and successfully applied in commercial batteries.[4,5] made it possible to establish the main rules governing ionic conductivity in NASICONs".

This sentence was corrected. We apologize for a formatting error.

In page 3 line 12, the authors should correct a word from "$Li_3Ti_2(PO_4)_2$" to "$LiTi_2(PO_4)_3$".

In the sentence (page 3 line 12): "Interestingly, transfer from M1 to M2 sites occurs simultaneously with lithium insertion and in the fully lithiated $Li_3Ti_2(PO4)_2$ all of the lithium occupies M2 sites." The cited composition stands for the fully lithiated form of the NASICON. This composition does not need to be corrected.

4. **Maybe some related works could supplement to enrich the paper: (1) Adv. Energy Mater. 2017, 1700247. (2) Nano Energy. 2016, 28, 224-231. (3) Chem. Mater., 2016, 28(18): 6553-6559.**

As suggested, references were added to the manuscript to broaden the introductory section.

Towards control over redox behaviour and ionic conductivity in $LiTi_2(PO_4)_3$ fast lithium-ion conductor

Wojciech Zając,[*a] Mateusz Tarach[a,b], Anita Trenczek-Zając[c]

[a] AGH University of Science and Technology, Faculty of Energy and Fuels, Department of Hydrogen Energy, Al. Mickiewicza 30, 30-059 Kraków, Poland.

[b] Instituto de Tecnología Química, Universidad Politécnica de Valencia – Consejo Superior de Investigaciones Científicas, Av. Naranjos s/n, E-46022 Valencia, Spain

[c] AGH University of Science and Technology, Faculty of Materials Science and Ceramics, Department of Inorganic Chemistry, Al. Mickiewicza 30, 30-059 Kraków, Poland

*corresponding author: e-mail: wojciech.zajac@agh.edu.pl, tel.: +48-12-6174751

Abstract

The location of redox couples in transition metal compounds is among the key factors that determine their applicability. $AM_2(PO_4)_3$ NASICONs (A = Na, Li; M = Ti, Zr, Hf, Ge, Sn, Fe, ...) form an intriguing group that feature fast ion diffusion and tunable reduction/oxidation potentials and can therefore find numerous applications. The present study focuses on the $LiTi_2(PO_4)_3$ member of this family and the possibility of controlling its transport and redox properties. It highlights the close relationship between the modification of the crystal and band structures via substitutions in the Ti sublattice or intercalation with lithium and its redox behaviour as well as transport properties. The correlation between ionic conductivity and the position of the Ti^{4+}/Ti^{3+} redox potential is discussed. UV-VIS reflectance spectra revealed a significant impact of the type of dopant as well as the level of intercalation on the position of the fundamental absorption edge, indicating the possibility of modifying the electronic structure. In the case of some of the examined dopants (Nb, Sn, In), more complex interaction was observed, since they introduce their own redox activity, and thus enable the material's behaviour to be modified even further.

Keywords: Electroceramics; Superionic conductor; Electrode potential; Optical spectroscopy; Li-ion battery.

Introduction

Along with energy production, energy storage is one of the key issues faced by modern civilization. Aside from portable electronics, energy grids and transportation are also expected to benefit considerably from improved electrochemical energy storage.[1] Prospective technologies comprise various types of supercapacitors and batteries. Progress in the performance, safety and cost of these systems largely depends on improvements in materials, especially electrodes and electrolytes. NASICON compounds, represented by the general formula $AM_2(XO_4)_3$ (A=Li,Na; M=Ti,Fe,V,Zr,…; X=P,Si,S), form an intriguing group of compounds. They were first discovered in 1970s by Goodenough et al.[2] Later, in 1980s Delmas et al.[3] observed reversible intercalation of alkali metal ions in $Na_{1+y}Ti_2(PO_4)_3$ compounds ($0 \leq y \leq 2$), indicating their electrochemical activity and applicability as electrode materials. Interestingly, due to growing interest in Na-ion batteries recent research efforts returned to NASICONs exhibiting reversible sodium incorporation. [4–6] Building on that knowledge, numerous polyanionic framework structures were proposed and successfully applied in commercial batteries.[7,8] Subsequent research made it possible to establish the main rules governing ionic conductivity in NASICONs.[9–11] It was found that it is the size of the tunnels through which mobile ions migrate that determines ionic mobility, and that the optimum tunnel size for Li^+ conduction is formed in the $LiTi_2(PO_4)_3$ crystal lattice. Ionic conductivity can be enhanced further by increasing the population of interstitial sites by the appropriate substitution of Ti^{4+} with aliovalent ions, such as Al^{3+}. This was reported to deliver one of the highest pure Li^+ conductivity values – up to $6 \cdot 10^{-3}$ S/cm at room temperature for

$Li_{1.3}Ti_{1.7}Al_{0.3}(PO_4)_3$.[12] The detailed description of NASICON crystal structure can be found elsewhere.[11,13–15] Briefly, there are two types of distinct sites for lithium (named M1 and M2) inside a skeleton formed by corner-sharing TiO_6 octahedra and PO_4 tetrahedra.[16] For stoichiometric $LiTi_2(PO_4)_3$, only M1 sites are populated, while the M2 ones remain vacant. Additional lithium ions can be inserted chemically or electrochemically and they settle into M2 sites. The occupation of M2 sites is thought to be essential for ionic diffusivity. Interestingly, transfer from M1 to M2 sites occurs simultaneously with lithium insertion and in the fully lithiated $Li_3Ti_2(PO_4)_2$ all of the lithium occupies M2 sites.[12,16] Similarly, increased temperature causes lithium to be transferred from M1 to M2 sites.[12,17]

In addition to alkali ion mobility, the location of redox couples in transition metal compounds is also a key factor that determines their applicability in electrochemical systems. Few water-stable materials offer as many possible applications as NASICONs.[18–22] It was found that polyanions actively participate both in the formation of the skeleton structure and the positioning of the $M^{n+}/M^{(n-1)+}$ redox potential through the inductive effect.[23,24] However, there are few papers that discuss the effect of aliovalent substitution at the M-site on the location of redox couples. López et al.[25] showed that the substitution of titanium with calcium raises the Ti^{4+}/Ti^{3+} potential by 0.3 V. Since the electrochemical intercalation of lithium involves both ionic and electronic components, a correlation between the electronic band structure of materials and its reduction (lithiation) potential is expected. In this work we investigate the relation between the partial substitution of Ti in $LiTi_2(PO_4)_3$ and its crystal structure, transport properties, and band structure as well as redox behaviour. The investigated substitutions include 3+ ions (Al^{3+}, Ga^{3+}, In^{3+}), 4+ ions (Ge^{4+}, Sn^{4+}, Zr^{4+}) and 5+ ions (Nb^{5+}) at concentrations of 0.3 mol per formula unit, for

a total of eight compositions: $LiTi_2(PO_4)_3$, $Li_{1.3}Ti_{1.7}M_{0.3}^{3+}(PO_4)_3$, $LiTi_{1.7}M_{0.3}^{4+}(PO_4)_3$ and $Li_{0.7}Ti_{1.7}M_{0.3}^{5+}(PO_4)_3$.

Experimental

$Li_{1.3}Ti_{1.7}M_{0.3}^{3+}(PO_4)^3$, $LiTi_{1.7}M_{0.3}^{4+}(PO_4)_3$ and $Li_{0.7}Ti_{1.7}M_{0.3}^{5+}(PO_4)_3$ samples were prepared using a high-temperature solid-state reaction. Stoichiometric amounts of Li_2CO_3 (99%, Acros Organics), $NH_4H_2PO_4$ (99.5%, Avantor Materials), TiO_2 (anatase, 99%, Aldrich), γ-Al_2O_3 (obtained through the decomposition of $Al(OH)_3$, 99.9%, Acros Organics), Ga_2O_3 (99.999%, Alfa Aesar), In_2O_3 (99.9%, Alfa Aesar), GeO_2 (99.99%, Alfa Aesar), SnO_2 (99.9%, Aldrich), ZrO_2 (99.5%, Alfa Aesar) and Nb_2O_5 (99.9%, Roth) were mixed and calcined at 275°C. The precursor powder was then homogenized in a Spex SamplePrep high-energy ball mill, pressed into pellets and fired at 900°C for 12 h.

Phase composition and crystal structure were investigated via X-ray diffraction, using the PANalytical Empyrean diffractometer with Cu K_α radiation filtered by means of nickel foil. The crystal structure parameters were calculated using the Rietveld method as implemented in the GSAS/EXPGUI software[26,27]. Ionic conductivity as a function of temperature was investigated via AC impedance spectroscopy, using the Solartron 1260 frequency response analyser, with an excitation voltage of 100 mV, and over the 1 MHz – 1 Hz frequency range. Prior to measurements, both sides of polished disk samples were covered with an Au paste, and the paste was fired at 850°C for 10 minutes. Impedance spectra were measured in air at temperatures ranging from ambient temperature to 200°C, in steps of 25°C.

The spectral dependence of the total reflectance (R_{tot}), consisting of specular and diffused reflectance, was measured using the Jasco V-670 UV-VIS-NIR double-beam spectrophotometer equipped with a 150 mm integrating sphere. Spectra were collected at room temperature over the range of 220-2200 nm, at the rate of 200 nm·min^{-1} and with a 0.5 nm step. Samples were placed in a powder holder with a quartz window. The thickness of the powder layer was sufficient to neglect transmittance, and it can thus be assumed that absorbance (A) equals A=1-R (R=0-1). The band-gap energy (E_g), which is associated with the optical transitions from the valence to the conduction band, was calculated from the Kubelka-Munk function[28,29], with an error of ±0.02 eV.

Chemical lithiation of $LiTi_2(PO_4)_3$ was carried out for a fine powder sample in a hexane solution and an argon atmosphere. A 0.5 M solution of n-butyllithium in n-hexane (Sigma Aldrich) was used as the lithiating agent. To ensure that the reaction was complete after $LiTi_2(PO_4)_3$ had been added, the suspension was stirred for 12h. The performed chemical lithiation can be represented as follows:

$$LiTi_2(PO_4)_3 + 2y\ C_4H_9Li \xrightarrow{n-hexane} y\ Li_3Ti_2(PO_4)_3 + \ (1-y)\ Li_1Ti_2(PO_4)_3 + y\ C_8H_{18} \qquad (1)$$

The obtained powder was then rinsed with n-hexane and dried. The amount of introduced lithium was controlled by adding a stoichiometric volume of an n-butyllithium solution.

Voltammetric analysis was carried out for $Li|Li^+|LiTi_2(PO_4)_3$-type cells in two-electrode R2032 stainless steel casings. Metallic lithium was used as a counter electrode. A 1 M $LiPF_6$ solution in ethylene carbonate and diethyl carbonate (EC/DEC=50/50 (v/v)) soaked in a fibreglass filter was applied as an electrolyte. The working electrode consisted of $LiTi_2(PO_4)_3$ mixed with carbon black (25 wt.%) and

polyvinylidene difluoride (5 wt.%) spread on aluminium foil. Voltammetric scans were run in the 1.2-4.0 V range using the Autolab PGSTAT 302N electrochemical analyser. During discharge, the electrochemical lithiation of $LiTi_2(PO_4)_3$ proceeded according to the following equation:

$$LiTi_2(PO_4)_3 + 2y\ Li^+ + 2y\ e^- \longleftrightarrow y\ Li_3Ti_2(PO_4)_3 + (1-y)\ Li_1Ti_2(PO_4)_3 \qquad (2)$$

Results and discussion

X-ray diffraction powder patterns for the obtained samples revealed a single-phase NASICON-type crystal structure with rhombohedral symmetry ($R\bar{3}c$ space group). Sharp peaks, e.g. full width at half maximum was 0.07° for $Li_{1.3}Ti_{1.7}Al_{0.3}(PO_4)_3$ at peak from (113) planes, indicated well-crystallized samples and allowed precise insight into the unit cell structure. In NASICONs, lattice parameters are controlled by at least two factors: the ionic radius of dopants and the population of M1 and M2 lithium sites. Fig. 1 depicts the relation between the dopant's ionic radius and *a*, *c* and unit cell volume values obtained via Rietveld refinement. For $LiTi_2(PO_4)_3$ with isovalent (4+) dopants in the Ti-site, a linear relation was observed, indicating unaffected Li- site occupancy. For 3+ dopants, for which the difference between the charge of the dopant and that of the host ion entails an increased number of lithium ions, the same type of dependence was preserved, although with a more gradual slope. This might be associated with changes in the electrostatic interactions in the crystal lattice, caused by altered occupancy of the M1 and M2 sites – perhaps the depopulation of M2 sites along with formation of vacancies at M1 sites; however, it is not possible to describe these effects quantitatively based on the obtained data alone. The observed trends are consistent with previous reports.[9,30] To the best of our knowledge, no detailed studies on the occupancy of lithium sites in $Li_{1-x}Ti_{2-x}Nb_x(PO_4)_3$

have been published; however, a significant expansion of both *a* and *c* as well as increased unit cell volume was observed when comparing these parameters with those reported for other dopants with a similar ionic radius. This may suggest that lithium does not undergo transfer to M2 sites and that the occupancy of M1 sites is decreased.

Impedance spectra measured for the studied samples were used to determine the bulk (grain interior) and grain boundary contributions to the ionic conductivity of the samples. The highest room temperature Li-ion bulk conductivity (1.7 mS cm^{-1}) and lowest activation energy (0.16 eV) was observed for $Li_{1.3}Ti_{1.7}Al_{0.3}(PO_4)_3$. The obtained values remain in agreement with previous reports.[9] All studied 3+ dopants yielded highly conducting samples with RT bulk conductivity in the range of 1.7 – 0.3 mS cm^{-1} and activation energies of 0.16 – 0.23 eV. As discussed by Pérez-Estébanez at al.,[12] the creation of vacant M1 sites together with the displacement of lithium into M2 sites upon the substitution of Ti with 3+ dopants increases the configurational entropy and, in consequence, the mobility of lithium ions. Aside from entropy contribution, the size of the bottlenecks which can be controlled via the ionic radius of a dopant also affects lithium mobility, as indicated by changes in activation energy. It seems that the optimum is reached for Al-doped $LiTi_2(PO_4)_3$. As 4+ dopants do not affect the occupancy of lithium sites, considerably lower bulk ionic conductivity ($4 \cdot 10^{-6} – 4 \cdot 10^{-7}$ S cm^{-1} at 30°C) and higher activation energy (0.27 – 0.51 eV) was observed for this group of compositions; nevertheless, also among 4+ dopants, the smallest Ge^{4+} ion provided the highest conductivity and the lowest activation energy, indicating that in this case bottleneck size is the most suitable for Li+ transport. The lowest Li^+ bulk conductivity among the studied samples, i.e. $8 \cdot 10^{-8}$ S cm^{-1} at room temperature, with a high activation energy (0.48 eV), was measured for the $Li_{0.7}Ti_{1.7}Nb_{0.3}(PO_4)_3$ sample.

This suggests that vacancies at M1 sites and bottleneck size are not the only factors that control transport properties; the displacement of excess lithium into M2 sites (as in the case of 3+ dopants) is also necessary to achieve a highly conducting NASICON material. A graphical comparison of all measured Li^+ conductivity values and the corresponding activation energies is presented in Fig. 2.

The electronic band structure and redox activity of materials are factors that are crucial for many applications, such as electronics, optics, photoelectrochemistry, catalysis, or electrochemical energy storage. The band structure of the investigated materials was studied by means of UV-VIS diffused reflectance spectroscopy. The obtained results are presented in Fig. 3.

For each of the studied materials, it was possible to identify an absorption edge in the UV range (300 – 400 nm), and for some of them the edge had a complex shape. The band gap was calculated using the Kubelka-Munk method, under the assumption that the optical transition is direct and allowed. The band gaps calculated for the main edges were between 3.52 and 3.74 eV, which indicates that these materials belong to the group of wide-band-gap semiconductors. Partial substitution of Ti^{4+} ions with Al^{3+}, Ga^{3+}, Ge^{4+}, and Zr^{4+} did not change the shape of the reflectance characteristics, but instead slightly shifted its position, suggesting that these elements remain electrochemically inert. When it came to In^{3+}, Sn^{4+} and Nb^{5+}, however, distinct two-edge absorption appeared, with a second band gap of 2.94 – 3.00 eV. The most pronounced change in the spectral dependence of R_{tot} was observed for the pentavalent Nb^{5+} dopant, for which the 3.6 eV band gap was hardly visible and all reflectance was red-shifted (3.11 eV). Interestingly, a smaller ionic radius of a doping ion or lower unit cell parameters resulted in an increased band gap, as in the case of III-V or II-VI semiconductors.[31] Furthermore, another concurrent trend was noted. Namely, the

altered population of lithium sites, as for 3+ dopants or Nb^{5+}, narrowed the band gap. For example, $Li_{1.3}Ti_{1.7}Ga_{0.3}PO_4$ with similar ionic radii of the host ion and the dopant and only slightly different unit cell parameters exhibited a significantly lower band gap when compared with the undoped material.

In order to test and verify the applicability of the observed fundamental relations, the entire series of investigated materials were examined in an electrochemical cell as working electrodes, which involved the transfer of both lithium ions and electrons. For such a process, a correlation between the crystal and electronic structure and reduction (lithiation) potential was to be expected.

Firstly, to investigate the evolution of the band structure of lithium titanium phosphate upon lithiation, five compositions at different stages of lithium insertion were prepared via the chemical reaction of $LiTi_2(PO_4)_3$ with n-butyllithium. The crystal structure of the lithiated powders was examined by means of X-ray diffraction. A selected region showing the evolution of the diffraction peak for reflex (113) is given in Fig. 4. It can clearly be seen that increased lithium content resulted in the formation of a new phase, $Li_3Ti_2(PO_4)_3$, which is distinct but isostructural with the initial compound and the $LiTi_2(PO_4)_3$:$Li_3Ti_2(PO_4)_3$ ratio gradually evolved from pure $LiTi_2(PO_4)_3$ to pure $Li_3Ti_2(PO_4)_3$. This observation leads to the conclusion that chemical lithiation of $LiTi_2(PO_4)_3$ NASICON proceeds via a two-phase mechanism. The same type of mechanism was observed for the electrochemical insertion of lithium. [32,33]

Diffuse reflectance spectra obtained for chemically lithiated $Li_{1+y}Ti_2(PO_4)_3$, in which y varies from 0 to 2, were obtained (Fig. 5). Lithiation leads to extensive changes in reflectance across the whole wavelength range, which is already clear at y = 0.5. Firstly, it was possible to notice that an increase in y during intercalation was accompanied by a shift in the fundamental absorption edge towards longer

wavelengths, indicating a decrease in the band gap and the appearance of a second, lower-energy transition in the 2.65 – 2.71 eV range. Moreover, the higher-energy transition disappeared for $y \geq 1.5$. Secondly, an additional absorption band was observed between 410 and 1200 nm – in the case of y = 0.5 – and in the range of 460 – 900 nm – for $y \geq 1$. Two minima of reflectance were observed at λ=562 and 690 nm. The new absorption bands can be explained by the presence of Ti^{3+} ions, which are electron colour centres, formed as a result of lithiation[34]. The band-gap energy values calculated for $Li_{1+y}Ti_2(PO_4)_3$ are shown in Fig. 5b. The higher-energy band gap initially decreased from 3.68 eV (y = 0) to 3.36 eV (y = 1) and subsequently faded away for $y \geq 1.5$. On the other hand, the lower-energy E_g slightly increased from 2.59 eV (y = 0) to 2.71 eV (y = 1.5). Two distinct band gaps that might be associated with two phases – $LiTi_2(PO_4)_3$ and $Li_3Ti_2(PO_4)_3$ – were observed in the X-ray diffraction patterns measured for lithiated samples during lithiation; the former was characterized by a higher band-gap energy, while the band-gap energy of the latter was lower by ca. 1 eV. The direction in which the band gap evolved remained consistent with the tendencies observed previously for changes of lattice parameters and occupancy of M1 and M2 lithium sites induced by dopants, as noted above – larger unit cell values and shift of lithium ions from M1 to M2 sites lead to a lower band gap. Lithiation might therefore be treated as another method of modifying the intrinsic properties of functional materials.

When reducing potential is applied to $LiTi_2(PO_4)_3$, the Ti^{4+} ions present in this compound can be reduced to Ti^{3+} with simultaneous incorporation of additional lithium ions. This process can be utilized and investigated in an electrochemical cell when $LiTi_2(PO_4)_3$ is used as an electrode against metallic lithium. Voltammograms showing cathodic (reduction) peaks are presented in Fig. 6a. According to Masquelier

and Croguennec, the Ti^{4+}/Ti^{3+} redox couple in $LiTi_2(PO_4)_3$ is located at 2.48 V vs. Li^+/Li.[7] In our study, we observed a cathodic peak for $LiTi_2(PO_4)_3$ cathode at 2.38 V, which is consistent with previous reports. Certain doping procedures, especially the partial substitution of titanium with 3+ elements like Al^{3+}, can improve bulk Li-ion conductivity by several orders of magnitude; however, there are no reports on the effect of dopants on electrochemical behaviour. The position of redox potential was therefore investigated for all studied materials: $LiTi_2(PO_4)_3$, $Li_{1.3}Ti_{1.7}M_{0.3}^{3+}(PO_4)_3$, $LiTi_{1.7}M_{0.3}^{4+}(PO_4)_3$ and $Li_{0.7}Ti_{1.7}M_{0.3}^{5+}(PO_4)_3$. Fig. 6b presents the location of the redox peak potential for the family of investigated materials.

It can be noted that – when charge of a dopant was constant – the reduction potential shifted towards lower (more reducing) potentials with decreasing dopant radius, which entails the contraction of the lattice. As with the previously discussed properties, the valence of the dopant also played important role in this case. Isovalent (4+) dopants resulted in the most negative potentials, 2.30 V vs. Li^+/Li. Aliovalent (3+ and 5+) dopants exhibited higher reduction potentials, up to 2.55 V for Nb^{5+}. The observed trend may be understood taking into account the fact that it closely follows the dependence of the band gap vs. the ionic radius of dopant and that the Ti^{3+} ion is larger than the Ti^{4+} ion, and a smaller space available for titanium ions should stabilize the charge state of Ti^{4+} against that of Ti^{3+}. The mobility of lithium seems to play a secondary role only. For a constant charge of the dopant, the highest Li^+ conductivity coincided with the most reducing redox potential; however, this trend was not sustained for all of the dopants. As discussed above, the occupancy of lithium sites strongly affects lithium mobility. The two-phase mechanism of insertion of lithium stands behind constant potential vs. reference related to the Ti^{4+}/Ti^{3+} redox couple resulting in a single peak in voltammograms. On the other hand, it seems that for

$Li_{0.7}Ti_{1.7}Nb_{0.3}(PO_4)_3$, beside Ti^{4+}/Ti^{3+}, another redox process appeared, as the second peak was observed. We guess that it could be related to a partial substitution of titanium with niobium and introduction of Nb^{5+}/Nb^{4+} ($Nb^{5+} + e^- = Nb^{4+}$) redox activity. We were not able to find any reports on redox processes related to Nb in the NASICON structure to support this statement, however, Patoux and Masquelier [33] showed that potential of lithium insertion into $NbPO_5$ coupled with Nb^{5+}/Nb^{4+} pair could be close to 2 V vs. Li^+/Li, which makes our guess plausible.

The correlation between the location of the reduction peak vs. band gap is presented in Fig. 7. The widest band gap corresponded to the lowest reduction potential – both were observed for the Ge-doped sample. Conversely, the opposite was noted for the Nb-doped NASICON.

Conclusions

Both the partial substitution of Ti^{4+} ions in $Li_xTi_{1.7}M_{0.3}(PO_4)_3$ with Al^{3+}, Ga^{3+}, In^{3+}, Ge^{4+}, Sn^{4+}, Zr^{4+} or Nb^{5+} and the intercalation of $Li_{1+y}Ti_2(PO_4)_3$ with Li^+ ions (y = 0 – 2) significantly affected the crystal and band structures of the investigated materials, resulting in ability of tuning ionic conductivity as well as optical and redox properties. For a constant charge of a dopant decreasing ionic radius resulted in decreased lattice constants, increased ionic conductivity, wider band-gap and Ti^{4+}/Ti^{3+} redox potential shifted towards more reducing potentials. However, these tendencies were overlapped and modified by the changes in occupancy of M1 and M2 lithium sites, which can be induced via doping at Ti-sublattice, or via intercalation with lithium. With increasing occupancy of M2 and decreasing occupancy of M1 sites Li^+ mobility increased, band gap decreased and Ti^{4+}/Ti^{3+} potential became less reducing.

Acknowledgements

This work was funded by the National Science Centre of Poland as part of the grant no. 2012/05/D/ST5/00472.

References

[1] Z. Yang, J. Zhang, M.C.W. Kintner-Meyer, X. Lu, D. Choi, J.P. Lemmon, Electrochemical energy storage for green grid, Chem. Rev. 111 (2011) 3577–3613.

[2] J.B. Goodenough, H.Y. Hong, J.A. Kafalas, Fast Na+-ion transport in skeleton structures, Mater. Res. Bull. 11 (1976) 203–220.

[3] C. Delmas, F. Cherkaoui, A. Nadiri, A Nasicon-type phase as intercalation electrode: $NaTi_2(PO_4)_3$, Mater. Res. Bull. 22 (1987) 631–639.

[4] J. Sheng, C. Peng, Y. Xu, H. Lyu, X. Xu, Q. An, L. Mai, $KTi_2(PO_4)_3$ with Large Ion Diffusion Channel for High-Efficiency Sodium Storage, Adv. Energy Mater. 2 (2017) 1–8.

[5] C. Xu, Y. Xu, C. Tang, Q. Wei, J. Meng, L. Huang, L. Zhou, G. Zhang, L. He, L. Mai, Carbon-coated hierarchical $NaTi_2(PO_4)_3$ mesoporous microflowers with superior sodium storage performance, Nano Energy. 28 (2016) 224–231.

[6] H. Gao, Y. Li, K. Park, J.B. Goodenough, Sodium extraction from NASICON-structured $Na_3MnTi(PO_4)_3$ through Mn(III)/Mn(II) and Mn(IV)/Mn(III) redox couples, Chem. Mater. 28 (2016) 6553–6559.

[7] C. Masquelier, L. Croguennec, Polyanionic (phosphates, silicates, sulfates) frameworks as electrode materials for rechargeable Li (or Na) batteries, Chem. Rev. 113 (2013) 6552–6591.

[8] J. Wang, X. Sun, Olivine $LiFePO_4$: the remaining challenges for future energy storage, Energy Environ. Sci. 8 (2015) 1110–1138.

[9] H. Aono, E. Sugimoto, Y. Sadaoka, N. Imanaka, G. Adachi, Ionic Conductivity of

Solid Electrolytes Based on Lithium Titanium Phosphate, J. Electrochem. Soc. 137 (1990) 1023.

[10] H. Aono, N. Imanaka, G. Adachi, High Li^+ Conducting Ceramics, Acc. Chem. Res. 27 (1994) 265–270.

[11] B. Lang, B. Ziebarth, C. Elsässer, Lithium Ion Conduction in $LiTi_2(PO_4)_3$ and Related Compounds Based on the NASICON Structure: A First-Principles Study, Chem. Mater. 27 (2015) 5040–5048.

[12] M. Pérez-Estébanez, J. Isasi-Marín, D.M. Többens, A. Rivera-Calzada, C. León, A systematic study of Nasicon-type $Li_{1+x}M_xTi_{2-x}(PO_4)_3$ (M: Cr, Al, Fe) by neutron diffraction and impedance spectroscopy, Solid State Ionics. 266 (2014) 1–8.

[13] D. Morgan, G. Ceder, Saïdi, J. Barker, J. Swoyer, H. Huang, et al., Experimental and Computational Study of the Structure and Electrochemical Properties of $Li_xM_2(PO_4)_3$ Compounds with the Monoclinic and Rhombohedral Structure, Chem. Mater. 14 (2002) 4684–4693.

[14] N. Bounar, A. Benabbas, F. Bouremmad, P. Ropa, J.-C. Carru, Structure, microstructure and ionic conductivity of the solid solution $LiTi_{2-x}Sn_x(PO_4)_3$, Phys. B Condens. Matter. 407 (2012) 403–407.

[15] D. Qui, Neutron powder diffraction study of solid solution $Li_{1+x}Ti_{2-x}In_xP_3O_{12}$ I. $0.0 \leq x \leq 0.4$, J. Solid State Chem. 72 (1988) 309–315.

[16] A. Aatiq, M. Menetrier, L. Croguennec, E. Suard, C. Delmas, On the structure of $Li_3Ti_2(PO_4)_3$, J. Mater. Chem. 12 (2002) 2971–2978.

[17] D.A. Woodcock, P. Lightfoot, Comparison of the structural behaviour of the low thermal expansion NZP phases $MTi_2(PO_4)_3$ (M = Li, Na, K), J. Mater. Chem. 9 (1999) 2907–2911.

[18] J.-Y. Luo, W.-J. Cui, P. He, Y.-Y. Xia, Raising the cycling stability of aqueous

lithium-ion batteries by eliminating oxygen in the electrolyte., Nat. Chem. 2 (2010) 760–765.

[19] Y. Cui, Y. Hao, W. Bao, Y. Shi, Q. Zhuang, Y. Qiang, Synthesis and Electrochemical Behavior of $LiTi_2(PO_4)_3$ as Anode Materials for Aqueous Rechargeable Lithium Batteries, J. Electrochem. Soc. 160 (2013) A53–A59.

[20] Z. Li, K.C. Smith, Y. Dong, N. Baram, F.Y. Fan, J. Xie, P. Limthongkul, W.C. Cartera, Y.-M. Chiang, Aqueous semi-solid flow cell: demonstration and analysis., Phys. Chem. Chem. Phys. 15 (2013) 15833–9.

[21] Z. Xiao, M. Ma, X. Wu, Z. He, S. Chen, Thin-film lithium-ion battery derived from Lil, Trans. Nonferrous Met. Soc. China. 16 (2006) 281–285.

[22] R. Kanda, M. Ogawa, T. Uemura, N. Ota, M. Ogawa, Solid-electrolyte battery, US 2012/0183834 A1, 2012.

[23] A.K. Padhi, K.S. Nanjundaswamy, C. Masquelier, J.B. Goodenough, Mapping of Transition Metal Redox Energies in Phosphates with NASICON Structure by Lithium Intercalation, J. Electrochem. Soc. 144 (1997) 2581–2586.

[24] A.K. Padhi, V. Manivannan, J.B. Goodenough, Tuning the Position of the Redox Couples in Materials with NASICON Structure by Anionic Substitution, J. Electrochem. Soc. 145 (1998) 1518–1520.

[25] M.C. López, G.F. Ortiz, P. Lavela, J.L. Tirado, R. Stoyanova, E. Zhecheva, Tunable Ti^{4+}/Ti^{3+} redox potential in the presence of iron and calcium in NASICON-type related phosphates as electrodes for lithium batteries, Chem. Mater. 25 (2013) 4025–4035.

[26] B.H. Toby, EXPGUI, A Graphical user interface for GSAS, J. Appl. Crystallogr. 34 (2001) 210–213.

[27] C.A. Larson, R.B. Von Dreele, General Structure Analysis System (GSAS), Los Alamos Natl. Lab. Rep. LAUR 86-74 (2004).

[28] P. Kubelka, F. Munk, Ein Beitrag zur Optik der Farbanstriche, Z. Tech. Phys. 12 (1931) 593–601.

[29] A.B. Murphy, Band-gap determination from diffuse reflectance measurements of semiconductor films, and application to photoelectrochemical water-splitting, Sol. Energy Mater. Sol. Cells. 91 (2007) 1326–1337.

[30] H. Aono, E. Sugimoto, Y. Sadaoka, N. Imanaka, G. Adachi, The Electrical Properties of Ceramic Electrolytes for $LiM_xTi_{2-x}(PO_4)_3+yLi_2O$, M = Ge, Sn, Hf, and Zr Systems, J. Electrochem. Soc. 140 (1993) 1827–1833.

[31] S. Adachi, Properties of Group-IV, II-V and II-VI Semiconductors, John Wiley & Sons Ltd, Chichester, England, 2005.

[32] C. Delmas, A. Nadiri, J. Soubeyroux, The nasicon-type titanium phosphates $ATi_2(PO_4)_3$ (A=Li, Na) as electrode materials, Solid State Ionics. 28–30 (1988) 419–423.

[33] S. Patoux, C. Masquelier, Lithium insertion into titanium phosphates, silicates, and sulfates, Chem. Mater. 14 (2002) 5057–5068.

[34] G. Dhanaraj, K. Byrappa, V. Prasad, M. Dudley, Handbook of crystal growth, Springer-Verlag Berlin Heidelberg, 2010.

*Figure1

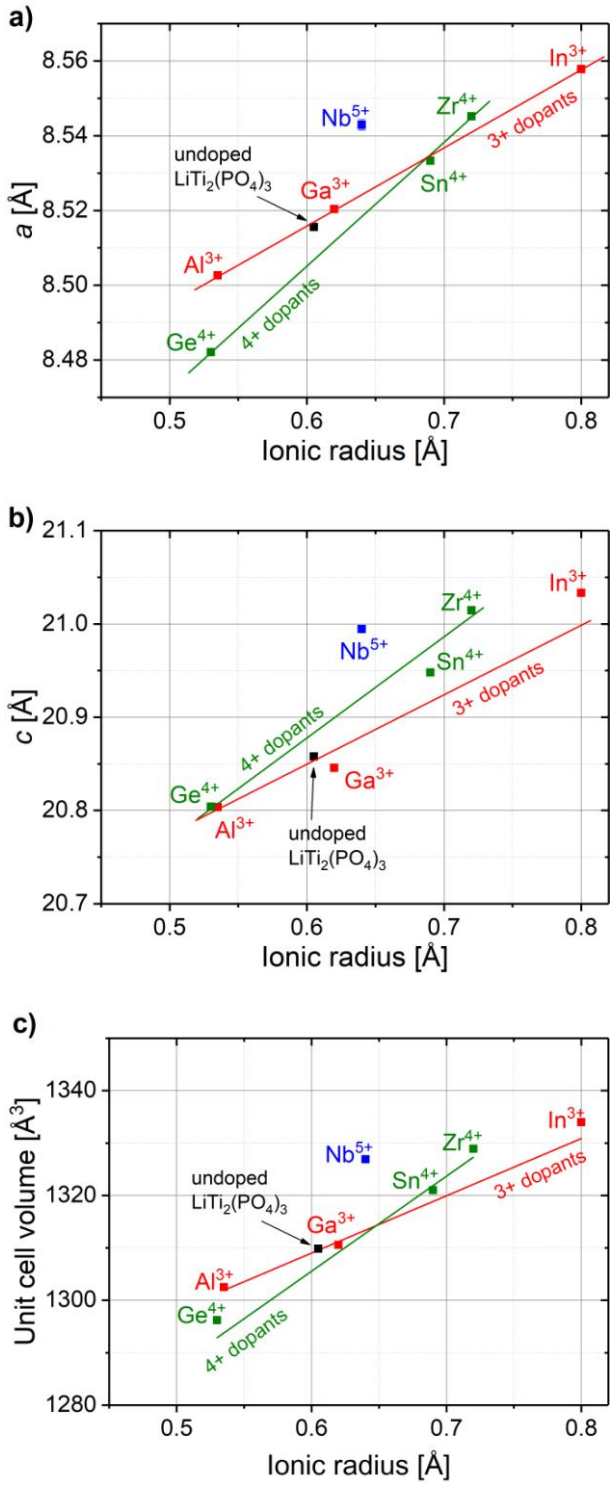

Fig. 1. Crystal lattice parameters for $LiTi_2(PO_4)_3$, $Li_{1.3}Ti_{1.7}M_{0.3}^{3+}(PO_4)_3$, $LiTi_{1.7}M_{0.3}^{4+}(PO_4)_3$ and $Li_{0.7}Ti_{1.7}M_{0.3}^{5+}(PO_4)_3$.

*Figure2

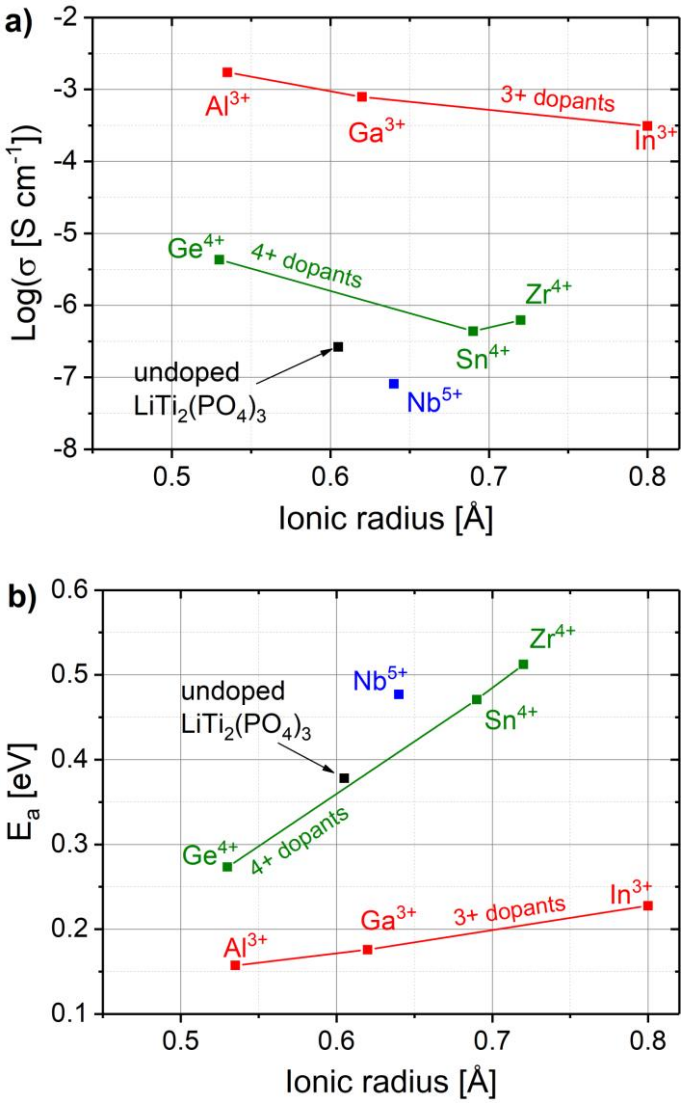

Fig. 2. (a) Li^+ bulk conductivity at 30°C and (b) its activation energy for $LiTi_2(PO_4)_3$, $Li_{1.3}Ti_{1.7}M_{0.3}^{3+}(PO_4)_3$, $LiTi_{1.7}M_{0.3}^{4+}(PO_4)_3$ and $Li_{0.7}Ti_{1.7}M_{0.3}^{5+}(PO_4)_3$.

*Figure3

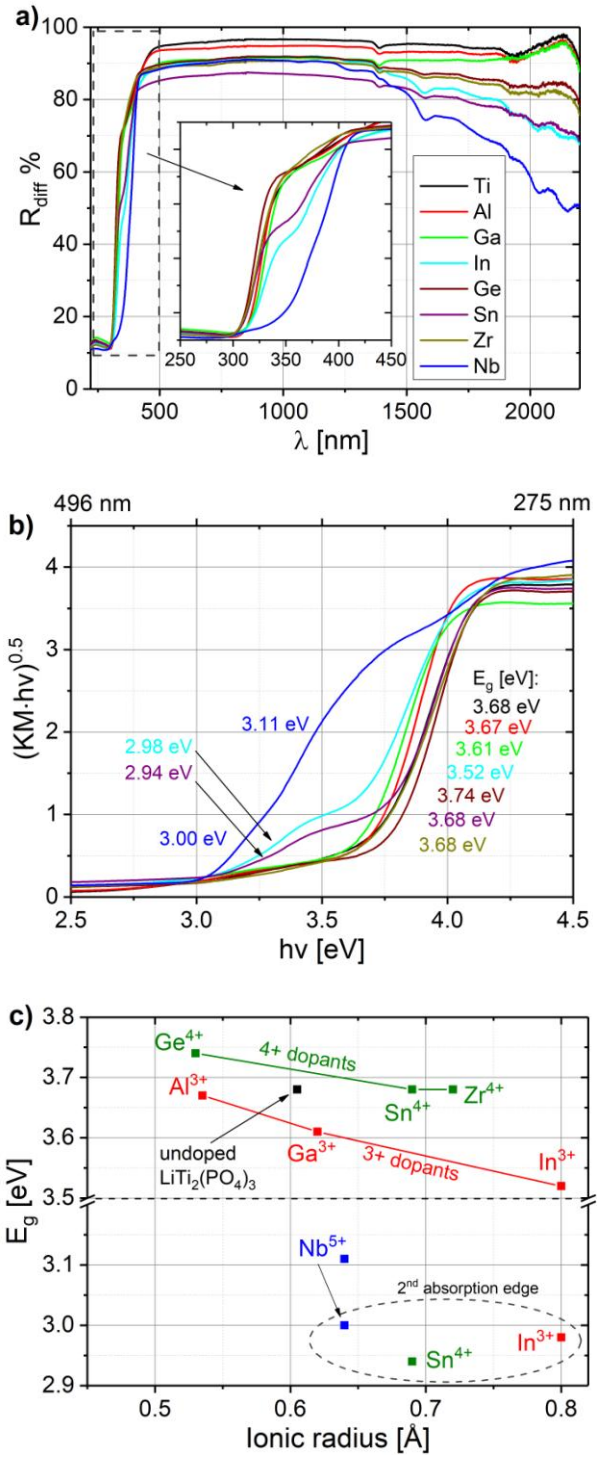

Fig. 3. Diffuse reflectance spectra of $LiTi_2(PO_4)_3$, $Li_{1.3}Ti_{1.7}M_{0.3}^{3+}(PO_4)_3$, $LiTi_{1.7}M_{0.3}^{4+}(PO_4)_3$ and $Li_{0.7}Ti_{1.7}M_{0.3}^{5+}(PO_4)_3$. (a) reflectance vs. wavelength, (b) Kubelka-Munk function vs. wavelength (band-gap energy values calculated from the Kubelka-Munk plot are displayed next to the spectra), (c) band-gap energy vs. ionic radius of the dopant.

*Figure4

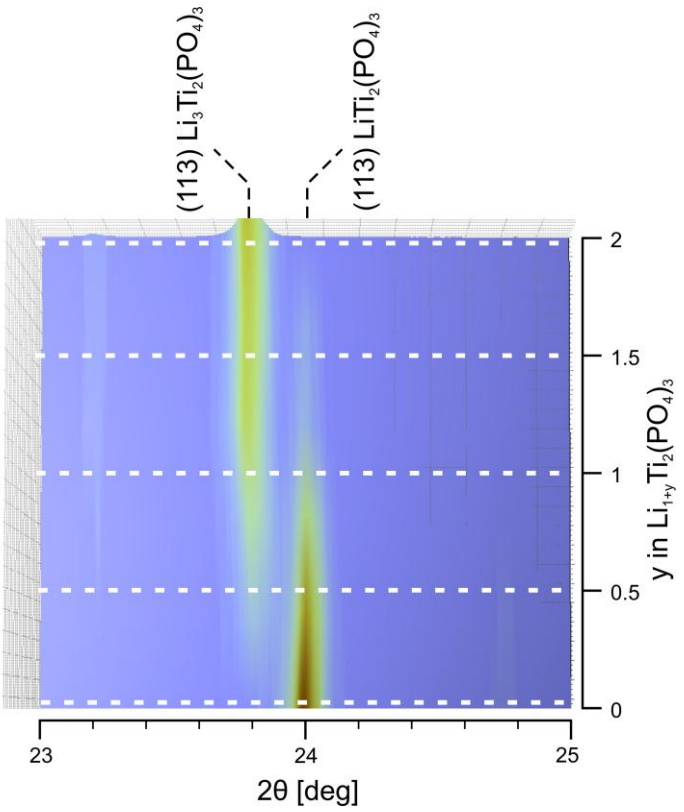

Fig. 4. Evolution of the (113) X-ray diffraction reflex during chemical lithiation. The average composition is given on the right vertical axis.

*Figure5

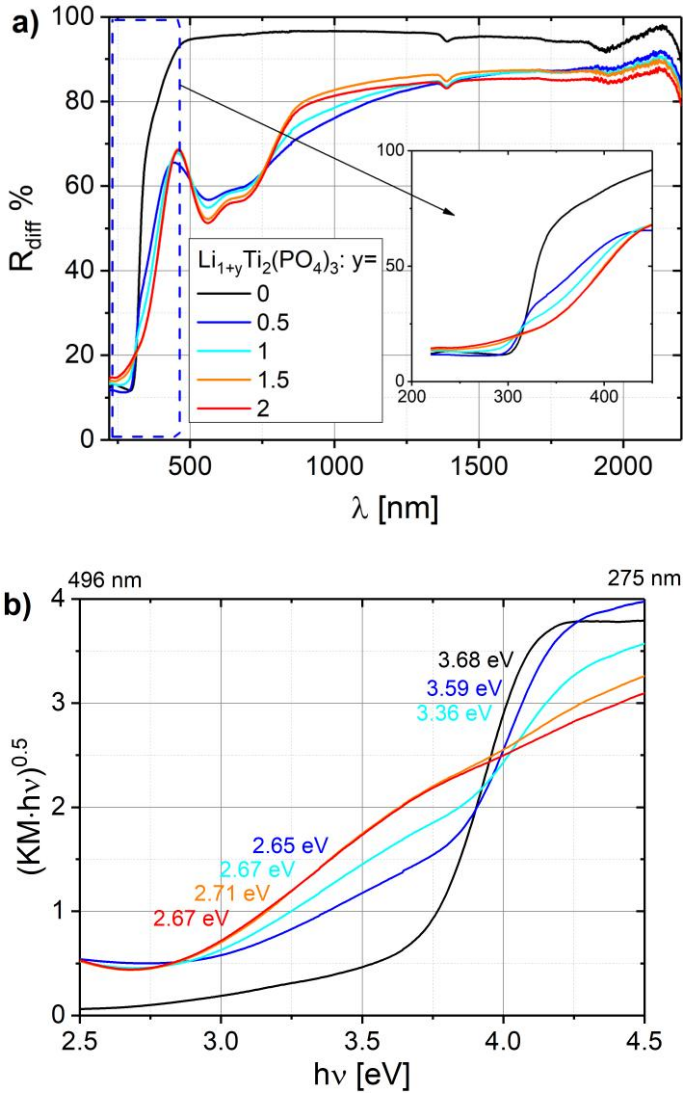

Fig. 5. Diffuse reflectance spectra for chemically lithiated $Li_xTi_2(PO_4)_3$. (a) Reflectance vs. wavelength, (b) Kubelka-Munk function vs. energy. Band-gap energy values calculated from the Kubelka-Munk plot are displayed next to the spectra.

*Figure6

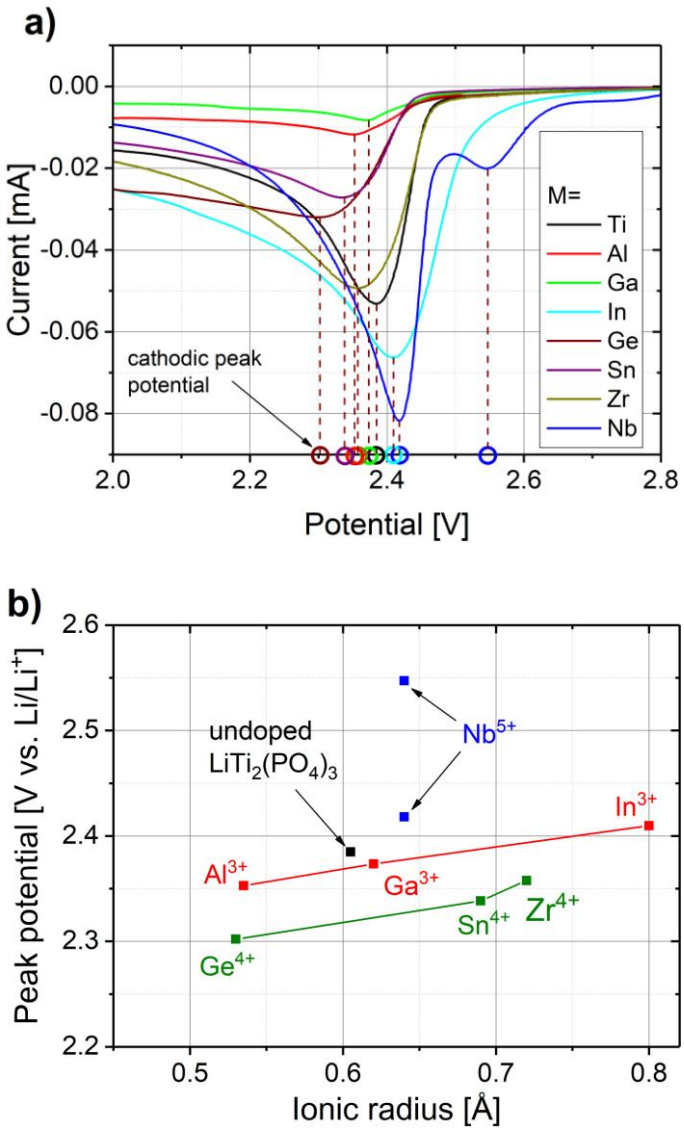

Fig. 6. (a) Voltammetric reduction curves, and (b) location of Ti^{4+}/Ti^{3+} reduction peak for $LiTi_2(PO_4)_3$, $Li_{1.3}Ti_{1.7}M_{0.3}^{3+}(PO_4)_3$, $LiTi_{1.7}M_{0.3}^{4+}(PO_4)_3$ and $Li_{0.7}Ti_{1.7}M_{0.3}^{5+}(PO_4)_3$.

*Figure7

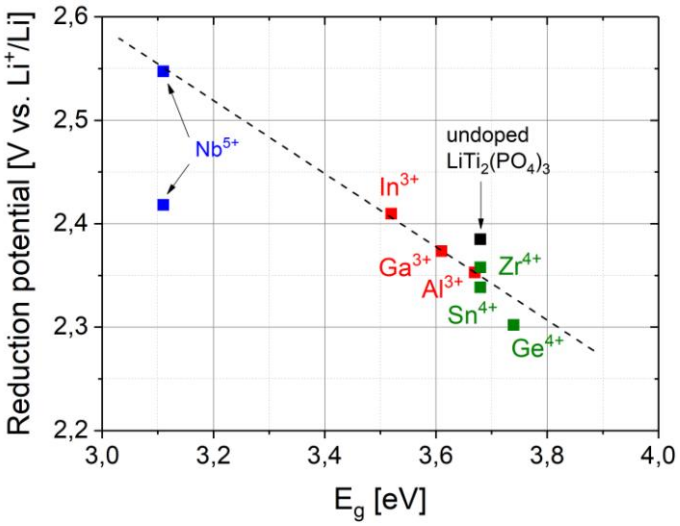

Fig. 7. (a) Reduction potential vs. band gap for $LiTi_2(PO_4)_3$, $Li_{1.3}Ti_{1.7}M_{0.3}^{3+}(PO_4)_3$, $LiTi_{1.7}M_{0.3}^{4+}(PO_4)_3$ and $Li_{0.7}Ti_{1.7}M_{0.3}^{5+}(PO_4)_3$.

*Graphical Abstract